

# Numerical Simulation of Supersonic Combustion Flows

In-Seuck Jeung<sup>\*†</sup> and Jeong-Yeol Choi<sup>\*\*</sup>

## 초음속연소유동의 수치해석연구

정인석<sup>\*†</sup> · 최정열<sup>\*\*</sup>

### ABSTRACT

Recently, renewed interest on the scramjet engine has been demonstrated through the many international activities along the several Asia-Pacific countries. Here, a short review of current activities on supersonic combustion in a scramjet engine will be addressed followed by the discussions on the review of numerical simulation on supersonic combustion phenomena related with scramjet engine combustors and ram accelerator. Emphasis was put on the grid refinement, scheme, unsteadiness and phenomenological differences.

**Key Words** : Supersonic Combustion, Scramjet Engine, Ram Accelerator, Cavity

### 1. Introduction

In the morning of 17 December 1903, Orville Wright made the first flight at about 10:35 am, a bumpy and erratic 12 seconds in the air. And then, Wilbur flew the plane 175 feet—just a few feet shorter than the wingspan of a Boeing 747. During the final flight of the day, piloted by Wilbur, the Wright Flyer remained airborne for 59 seconds and flew 852 feet.[1] About 100 years later, in 30 July 2002, the world first scramjet combustor, HyShot flight test payload, demonstrated a successful supersonic combustion during hypersonic flight of Mach 7.7 for 5 seconds flying about 12 km.[2] Soon, in 27 March 2004, NASA made the first successful hypersonic flight of Mach 6.8 by X-43A hypersonic airplane installed a scramjet engine for 10 seconds of powered flight, and again in 16 November 2004, made the second successful hypersonic flight accelerated from Mach 6.8 to 9.8.[3]

Even though, there are so many important issues related with better understandings on the supersonic combustion phenomena in the scramjet engine, we limit our topics only on the effect of grid refinement, scheme unsteadiness, and phenomenological differences on the solution quality of numerical simulation onto supersonic combustion. For these purposes, we selected the case of numerical simulation for the HyShot scramjet combustor with a poor grid of coarse spacing[4], second case for a virtual scramjet engine composed by a straight/divergent flow path with/without cavity area of a good grid system of fine spacing[5], and finally third case of a ram accelerator for the superdetonative mode flight speed, which was filled by Hydrogen-air/diluted by Nitrogen combustible premixed gas.[6] It is believed that first case and second case would be controlled by turbulent mixing limited, while third case would be controlled by reaction limited.

\* 서울대학교 항공우주공학과

† 연락처자, E-mail : enjis@snu.ac.kr

\*\* 부산대학교 항공우주공학과

## 2. Computational Formulations and Algorithms

### 2.1 Conservation Equations

The combustor configuration is assumed to be two dimensional for computational efficiency. The conservation equations for a multi-component system are employed to analyze the chemically reacting flow in a scramjet combustor. The coupled form of the species conservation equations, fluid dynamics equations, and turbulent transport equations can be summarized in a conservative vector form as follows.

$$\frac{\partial \mathbf{Q}}{\partial t} + \frac{\partial \mathbf{F}}{\partial x} + \frac{\partial \mathbf{G}}{\partial y} = \frac{\partial \mathbf{F}_v}{\partial x} + \frac{\partial \mathbf{G}_v}{\partial y} + \mathbf{W}$$

where the conservative variable vector,  $\mathbf{Q}$ , convective flux vectors,  $\mathbf{F}$  and  $\mathbf{G}$ , diffusion flux vectors,  $\mathbf{F}_v$  and  $\mathbf{G}_v$ , and reaction source term  $\mathbf{W}$  are defined. Details of the governing equations and thermal properties are described in the literature[8].

$$\mathbf{Q} = \begin{bmatrix} \rho_i \\ \rho u \\ \rho v \\ \rho e \\ \rho k \\ \rho \omega \end{bmatrix} \quad \mathbf{F} = \begin{bmatrix} \rho_i u \\ \rho u^2 + p \\ \rho uv \\ \rho H u \\ \rho k u \\ \rho \omega u \end{bmatrix} \quad \mathbf{G} = \begin{bmatrix} \rho_i v \\ \rho uv \\ \rho v^2 + p \\ \rho H v \\ \rho k v \\ \rho \omega v \end{bmatrix}$$

$$\mathbf{F}_v = \begin{bmatrix} -\rho_i u_i^d \\ \tau_{xx} \\ \tau_{xy} \\ \beta_x \\ \mu_k \partial k / \partial x \\ \mu_\omega \partial \omega / \partial x \end{bmatrix} \quad \mathbf{G}_v = \begin{bmatrix} -\rho_i u_i^d \\ \tau_{xy} \\ \tau_{yy} \\ \beta_y \\ \mu_k \partial k / \partial y \\ \mu_\omega \partial \omega / \partial y \end{bmatrix} \quad \mathbf{W} = \begin{bmatrix} w_i \\ 0 \\ 0 \\ 0 \\ s_k \\ s_\omega \end{bmatrix}$$

### 2.2 Combustion Mechanism and Turbulence Closure

The present analysis employs the GRI-Mech 3.0 chemical kinetics mechanism for hydrogen-air combustion [7]. The mechanism consists of eight reactive species (H, H<sub>2</sub>, O, O<sub>2</sub>, H<sub>2</sub>O, OH, H<sub>2</sub>O<sub>2</sub> and HO<sub>2</sub>) and twenty-five reaction steps. Nitrogen is assumed as an inert gas because the oxidation process does not

have significant effect on the fluid dynamics in a combustor. Turbulence closure is achieved by means of Mentor's SST (Shear Stress Transport) model which is based on the k- $\omega$  two-equation formulation [8]. This model is the blending of the standard k- $\epsilon$  model that is suitable for a shear layer problem and the Wilcox k- $\omega$  model that is suitable for wall turbulence effect[9]. Baridna et al. reported that the SST model shows good prediction for mixing layer and jet flow problems, and that it is also less sensitive to initial values [10]. In the case of ram accelerator calculation simple Baldwin-Romax model was employed.

Another important issue is the closure problems for the interaction of turbulence and chemistry in supersonic conditions. Recently, there were many attempts to address this issue using LES methods, PDF approaches, and other combustion models extended from subsonic combustion conditions. Although much useful advances were achieved, the improvement was significant in comparison with the results from laminar chemistry and existing experimental data, as evidenced in the results by Möbus et al [11]. By examining the existing results, such as Norris and Edwards [12], it is thought that the solution accuracy seems to be more dependent on grid resolution than the modeling of turbulence-chemistry interaction. In view of the lack of reliable models for turbulence-chemistry interactions, especially for supersonic flows, the effect of turbulence on chemical reaction rate is ignored in the present work.

### 2.3 Computational Algorithms

The governing equations were discretized numerically by a finite volume approach. The convective fluxes were formulated using Roe's FDS method derived for multi-species reactive flows along with the MUSCL approach along with a differentiable limiter function. The spatial discretization strategy satisfies TVD conditions and shows high-resolution shock capturing capability. The discretized equations were temporally integrated using a second-order accurate fully implicit method. A Newton sub-iteration method was also used to preserve the time accuracy and solution

stability. Since detailed descriptions of the governing equations and numerical formulation are documented in the previous literature [13], it will not be recapitulated here. The numerical methods have been validated against a number of steady and unsteady simulations of shock-induced combustion phenomena that showed good agreement with existing experimental data [14-15].

### 3. HyShot Scramjet Combustor

#### 3.1 Combustor Configuration

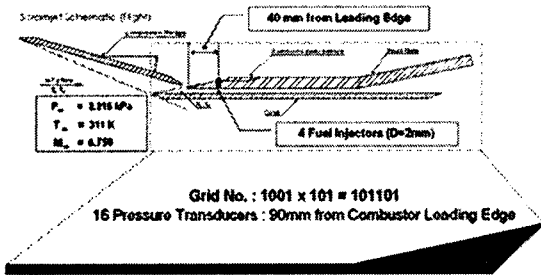


Fig. 1 HyShot Geometry

HyShot scramjet combustion flow path is shown in Fig.1. The channel type combustor of 9.8mm height, 75mm width, and 300mm length is composed of transverse fuel injection and constant area straight duct[16]. The incoming airflow to the combustor inlet is set to Mach number 2.74 at 1256K and 83.48 kPa. Grid spreading over this combustor section is 1001 x 101.

#### 3.2 Results

Fig. 2 shows calculated results of temperature distribution and OH distribution. Results showed clearly transverse fuel injection, upstream subsonic flow separation and wavy large scale mixing along the flame front. However, when it is compared with experimental case, as shown in Fig. 3, numerical result is thought as the sequence of less mixing than actual experimental case. We can notice that pressure distribution predicted numerical simulation along the combustor for the case of equivalence ratio  $\phi=0.786$  is about same level as those of experimental case  $\phi=0.621$ .

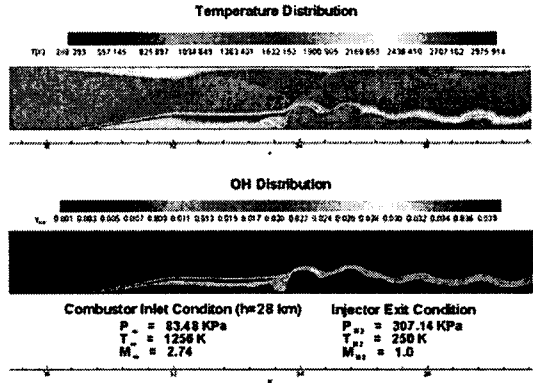


Fig. 2 Temperature & OH Concentration Distribution

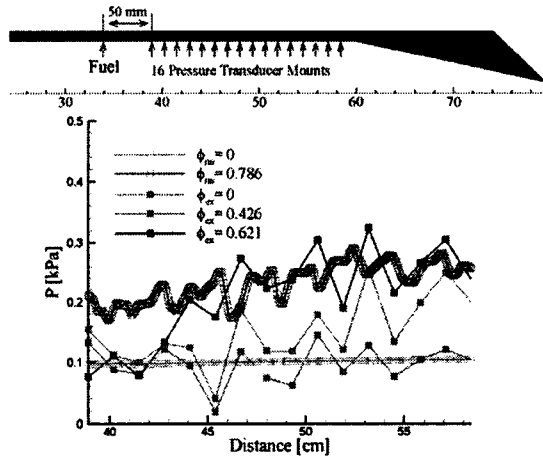


Fig. 3 Pressure Distribution

### 4. Configuration of Scramjet Combustor

#### 4.1 Combustor Configuration

The supersonic combustor considered in this study is shown in Fig. 4. The channel type combustor of 10 cm height and 131 cm length is composed of transverse fuel injection and a cavity. This combustor configuration is quite similar to the HyShot test model, except for the cavity, in which a swallowing slot is employed to remove the boundary layer from the inlet and the combustor starts with a sharp nose [16]. A cavity of 20 cm length and 5cm depth, having an aspect ratio, L/D of 4.0, is employed at 20 cm downstream of the

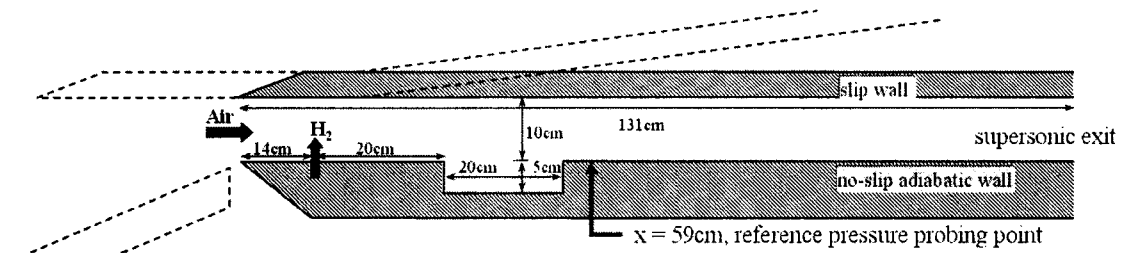


Fig. 4 Scramjet Combustor Configuration

injector.

#### 4.2 Operating Conditions

The incoming air flow to the combustor is set to Mach number 3 at 600 K and 1.0 MPa. This combustor inlet condition roughly corresponds to a flight Mach number 5-6 at an altitude of 20 km, although the exact condition depends on the inlet configuration. Gaseous hydrogen is injected vertically through a slot of 0.1 cm width to the combustor through a choked nozzle. The fuel temperature is set to 151 K. The injector exit pressures are 0.5, 1.0 and 1.5 Mpa, and the overall equivalence ratios are 0.167, 0.33 and 0.5.

#### 4.3 Combustor Conditions

A total of  $936 \times 160$  grids are used for the main combustor flow passage, and  $159 \times 161$  grids for the cavity. The grids are clustered around the injector and the solid surfaces and the injector. 54 grid points are included in the injector slot and the minimum grid size near the wall is  $70 \mu\text{m}$ . All the solid surfaces are assumed to be no-slip and adiabatic, except for the upper boundary. For convenience and reduction of the number of grid points required to resolve the boundary layer, the upper boundary is assumed to be a slip wall, which is equivalent to the flow symmetric condition in the present configuration. Extrapolation is used for the exit boundary. Time step is set to 6 ns according to the minimum grid size and the CFL number of 2.0. Four sub-iterations are used at each time step. Figure 2 is a magnified plot of the computational grid around the injector and the fore part of the cavity shown as a dashed-box in Fig. 1.

#### 4.4 Results

Numerical simulations were carried out for twelve cases, including non-reacting and reacting flows, with/without cavity for three different injection pressures of 0.5, 1.0 and 1.5 MPa. The following sections will discuss the results for each case. All the cases were run for 6 ms starting from the initial condition, which is longer than the typical test time of the ground based experiments. The plots of the instantaneous flow fields shown in the followings were taken at 5 ms.

##### 4.4.1 Non-reacting Flows Without Cavity

Instantaneous temperature fields for the cases of nonreacting flows without a cavity are plotted in Fig. 5. For the injection pressure ratio of 5.0, the flow field around the injector seems to be quite stable, but a flow disturbance is observed at the location around 40 cm where the first reflected shock wave interacts with the shear layer between the fuel and air flows. The disturbance propagates upstream through the shear layer, but can not reach the injector. Thus the injector flow remains stable and the fuel flow is located very close to the lower surface. The mechanism of the shear layer instability, which is triggered by the impinging oblique shock wave, seems to be the one studied by Papamoschou and Roshko[17]. For the injection pressure ratio of 10.0, disturbance was generated during the early stage of the computation in a manner similar to the case of the injection pressure ratio of 5.0. However the disturbance propagates upstream and triggers the injector flow to become unstable. As a result of this interaction, a large portion of the flow area becomes subsonic and the injector flow oscillates strongly. This unstable motion

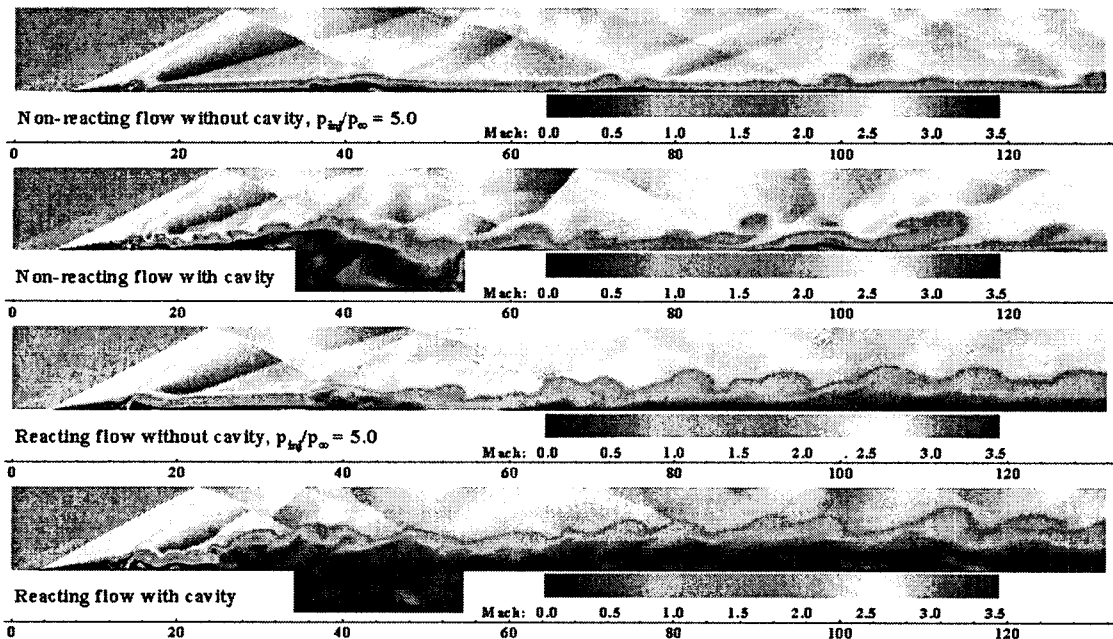


Fig. 5 Mach Number Field

leads to a higher fuel penetration and the fuel/air mixing is strongly enhanced. This injector flow instability mechanism has been observed by Papamoschou and Hubbard [18]. Ben-Yakar et al. also observed essentially the same unstable injection jet in their supersonic combustion experiment [19]. For the injection pressure ratio of 15.0, the injector flow instability is getting stronger and oscillatory flows are observed in the entire combustor field. Thus the fuel penetrates around the middle of the combustor and the fuel/air mixing is greatly enhanced.

#### 4.4.2 Non-reacting Flows With Cavity

Figure 5, again, shows the instantaneous temperature fields for the case of non-reacting flows with a cavity. The cavity plays an important role in disturbing the flow field and mixing the fuel and air. What is different from the cases without cavity is that the cavity generates disturbances which in turn trigger the injector flow to become unstable even for the case with a low injection pressure ratio of 5.0. Thus, the injector flow becomes unstable for all the pressure ratios under conditions with a cavity. The fuel penetration and fuel/air mixing seems to be enhanced by the

oscillating mechanism of the cavity. For all the three injection pressure ratios, the injector instability is triggered by the cavity induced instability within 1 ms, which is around the half of the value for the cases without a cavity. Also the pressure fluctuation is much stronger and the pressure level is maintained slightly higher than the cases without a cavity. The expected cavity oscillation frequencies from Rossiter's semi empirical formula discussed by Ben-Yakar and Hanson [20] are 1.9 kHz for the first mode and 4.5 kHz for the second mode for the flow conditions in this study. Thus the present for the flow conditions in this study.

#### 4.4.3 Reacting Flows Without Cavity

Subsequently, the instantaneous temperature fields for reacting flows without a cavity. For the injection pressure ratio of 5.0, combustion occurs in the frontal separation region, but is not fully established along the shear layer. This separation region contains a pool of radicals and acts as a preheating zone. The flame is not anchored there, but in the region containing shock-wave/shear-layer interaction where the instability is generated. Downstream of this location, heat release from chemical

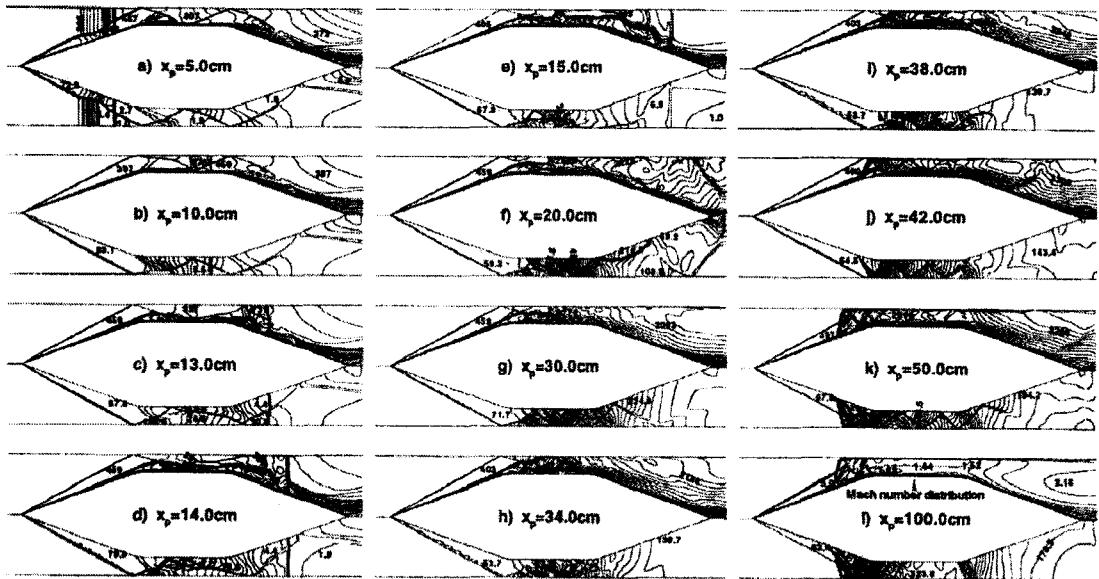


Fig. 6 Temperature Distributions(upper half of each figures) and Pressure Distributions (lower half of each figures) in Marching Sequence for  $2\text{H}_2+\text{O}_2+5\text{N}_2$  Mixture. Mach number distributions are plotted for the case after  $x_p=100.0\text{cm}$

reactions takes place, accompanied with large vortices convecting downstream. The overall phenomena seem quite similar to a typical turbulent diffusion flame generating large vorticities. It is thought from this result that chemical reactions do not intensify the disturbance to an extent sufficient for triggering the instability of the injector flow. For the injection pressure ratios 10.0 and 15.0, the temperature fields show different characteristics. Due to the large heat release, the pressure behind the injector builds up and leads to a Mach reflection across the combustor. A large subsonic region is formed downstream of the injector, and the injector flow no longer shows a structure composed of a leading oblique shock wave, a frontal separation region, etc. Instead, the fuel is injected through a narrow width of subsonic jet, but can penetrate much deeper. The frontal separated flow region, which has a role as a radical pool and a pre-heater, still exists for the injection pressure ratio of 10.0, but disappears

## 5. Configuration of Ram Accelerator

Ram Accelerator is a novel concept using a

principle of ramjet propulsion as a propelling mechanism of a projectile similar to the LEO satellite in a barrel, so a combustible mixture gas is compressed by a series of shocks and then generates thrust force, consequently in a similar way as Oblique Detonation Wave Engine(ODWE) or scramjet engine.

One of an example is listed here for a projectile of 28mm diameter, and 220mm length flying inside the barrel of 40mm diameter. Flow condition is such as initial combustible fill pressure of 25atm hydrogen/oxygen/diluent gas mixture at 300K, projectile highest Mach number 6-7. Mainly 400 x 60 grid is used, while grid refinement test has been done for the case of 800 x 120 and 1600 x 240 grids. Quasi-Steady wall pressure distribution for the case of  $2\text{H}_2+\text{O}_2+7\text{N}_2$  mixture is tested, and shows almost same results. In Fig. 10, flow development around flying projectile is shown along the height distance until 100cm elapsed. We can notice shock waves, boundary layer, separation bubble, shock-induced combustion detonation waves, and global flow field considerably realistically. It may be said that less fine grid system still works not losing any important flow physics hence numerical simulation for premixture supersonic

combustion is less sensitive to the grid spacing. It is thought premixture combustion is basically reaction controlled phenomena but not mixing controlled phenomena as previously shown for the case of scramjet combustion.

## 6. Summary

The reacting flow dynamics in a scramjet combustor was carefully studied by means of a comprehensive numerical analysis. The present results show a wide range of phenomena resulting from the interactions among the injector flows, shock waves, shear layers, and oscillating cavity flows. As a conclusion of the present study, new findings can be summarized as follows.

- 1) Strong unsteady flow characteristics were identified for a scramjet combustor. The work appears to be the first of its kind in the numerical study of combustion oscillations in a supersonic combustor.
- 2) Large flow disturbances can be generated by shear layer instability that may be triggered by the interactions with shock waves.
- 3) For all the cases studied herein, instability caused by the cavity seems to override the shear layer instability caused by the shock-wave/shear-layer interactions when both instabilities are present.
- 4) Transverse injected jet may remain stable without disturbance, but can be triggered to become unstable with disturbances from a shear layer or a cavity. Disturbed transverse injected jet has deeper penetration and improved fuel/air mixing than the stabilized one. A more careful study is necessary to characterize the stability of transverse injection jets.
- 5) The roles of the cavity as a source of disturbance for the transverse jet, fuel/air mixing enhancement, and flame holder were clarified.
- 6) Unstable flow characteristics for the reacting cases are similar to that of non-reacting flows except for the cases where pressure builds up rapidly.
- 7) As an extreme case of high pressure build up, thermal choking of the combustor was observed, which resulted in the combustor unstart by the forward running strong shock wave.
- 8) Variable geometry can mitigate thermal choking, hence enhance combustor operation range.
- 9) Boundary layer development and flow separation are very importantly effecting to the onset of thermal choking.
- 10) Adequate numerical grid refinement is seriously demanded.
- 11) Premixed combustion simulation has less sensitive to the grid spacing.

## 7. Acknowledgments

This research was partly supported by National Research Laboratory program(M10500000072-05J000007210). The authors wish to acknowledge this financial support.

## Reference

- [1] Celebrating a Century of Flight, *NASA Publication SP-2002-09-511-HQ*, 2002, 6-7.
- [2] Dornheim, M. A., Australian Scramjet Flight Should bolster Research Database, *Aviation Week and Space Technology*, August 5, 2002, 30-31
- [3] National Reports HyShot, Japanese Programs, and AIAA Paper 2005-3315 -3317, -3318, *Proceedings of the 13th AIAA/CIRA International Space Planes and Hypersonic Systems and Technologies Conference*, May 16-20, 2005.
- [4] Won, S.H., Jeong, E, Jeung, I.S. and Choi, J.Y., Numerical Simulation Study on Combustion Characteristics of Hypersonic Model SCRamjet Combustor, *Proceedings of Asian Joint Conference on Propulsion and Power*, 4-6 March, 2004, 42-47.
- [5] Choi, J.Y., Unsteady Combustion Phenomena in Scramjet Combustor, *Proceedings of the 2005 KSPE Spring Conference*, 22-23 April, 2005, 364-367.
- [6] Choi, J.Y., Jeung, I.S. and Yoon, Y., Numerical Study of Scram Accelerator Starting Characteristics, *AIAA Journal*, 37(5), 1999, 537-543.
- [7] Smith, G. P., Golden, D. M., Frenklach, M., Moriarty, N. W., Eiteneer, B., Goldenberg, M., Bowman, C.T., Hanson,

- R.K., Song, S., Gardiner Jr., W.C., Lissianski, V.V., and Qin, Z., GRIMech, [http://www.me.berkeley.edu/gri\\_mech/](http://www.me.berkeley.edu/gri_mech/)
- [8] Menter, F. R., Two-Equation Eddy-Viscosity Turbulence Models for Engineering Application, *AIAA Journal*, 32(8), 1994, pp.1598-1605.
- [9] Wilcox, D. C., Turbulence Modeling for CFD, DCW Industries, La Cañada, CA, 1993.
- [10] Bardina, J. E., Huang, P. G., and Coakly, T. J., Turbulence Modeling Validation, AIAA 97-2121, 1997.
- [11] Möbus, M., Gerlinger, P. and Brüggermann, Scalar and Joint scalar-Velocity-Frequency Monte Carlo PDF simulation of Supersonic Combustion, *Combustion and Flame*, 132(1), 2003, pp.3-24.
- [12] Norris, J. W. and Edwards, J. R., Large-Eddy Simulation of High-Speed Turbulent Diffusion Flames with Detailed Chemistry, AIAA Paper 97-0370, 1997.
- [13] Choi, J.-Y., Jeung, I.-S. and Yoon, Y., "Computational Fluid Dynamics Algorithms for Unsteady Shock-Induced Combustion, Part 1: Validation," *AIAA Journal*, 38(7), 2000, 1179-1187.
- [14] Choi, J.-Y., Jeung, I.-S. and Yoon, Y., Unsteady- State Simulation of Model Ram Accelerator in Expansion Tube, *AIAA Journal*, 37(5), 1999, 537-543.
- [15] Choi, J.-Y., Jeung, I.-S. and Yoon, Y., Scaling Effect of the Combustion Induced by Shock Wave/ Boundary Layer in Premixed Gas, *Proceedings of the Combustion Institute*, 27, 1998, 2181-2188.
- [16] Centre for Hypersonics HyShot Scramjet Test Programme, <http://www.mech.uq.edu.au/hyper/hvshot/>
- [17] Papamoschou, D., and Roshko, A., The Turbulent Compressible Shear Layer: An Experimental Study, *Journal of Fluid Mechanics*, 197, 1988, 453-477.
- [18] Papamoschou, D., and Hubbard, D.G., Visual Observations of Supersonic Transverse Jets, *Experiments in Fluids*, 14(5), 1993, 468-471., <http://supersonic.eng.uci.edu/scramjet.htm>
- [19] Ben-Yakar, A., Kamel, M .R., Morris, C. I. and Hanson, R. K., Experimental Investigation of H<sub>2</sub> Transverse Jet Combustion in Hypervelocity Flows, AIAA Paper 97-3019, 1997.
- [20] Ben-Yakar, A. and Hanson, R. K., Cavity Flame-Holders for Ignition and Flame Stabilization in Scramjets: An Overview, *Journal of Propulsion and Power*, 17(4), 2001, 869-877.